THE JOURNAL OF PHYSICAL CHEMISTRY A
A JOURNAL OF THE AMERICAN CHEMICAL SOCIETY

pubs.acs.org/JPCA Article

Mechanism of Orbital Interactions in the Sharpless Epoxidation with Ti(IV) Peroxides: A DFT Study

Robert D. Bach* and H. Bernhard Schlegel

Cite This: https://doi.org/10.1021/acs.jpca.1c08447 Read Online

ACCESS | Metrics & More | Article Recommendations | Supporting Information

ABSTRACT: The M06-2X DFT functional has been employed to examine monomeric titanium(IV) hydroperoxo catalysts that model the individual steps in the dimeric titanium(IV)-catalyzed Sharpless reaction. This is the first example of a transition structure for titanium(IV) *tert*-butyl hydroperoxide-catalyzed epoxidation that describes the molecular motion required for oxygen atom transfer. These epoxidation catalysts have been examined for both bimolecular reactions with E-2-butene and the intramolecular epoxidation of allyl alcohol. The transition structure for the bimolecular peroxyacetic acid epoxidation of E-2-butene has been shown to be spiro in nature, and likewise, the intramolecular epoxidation of allyl alcohol is also nearly spiro. The significance of the O−C−C═C dihedral angle of allyl alcohol is examined for the Ti(IV) *tert*-butyl hydroperoxide epoxidation mechanism. Evidence is presented that supports a hexacoordinate titanium peroxo environment that exists in the dimeric form of the Sharpless catalyst. The mechanism for a 1,3-rearrangement of the alkoxide ligand in a titanium hydroperoxide to the Ti center in concert with oxygen atom transfer of the proximal oxygen to the C═C bond of the substrate is presented. The dimerization of Ti(IV)-(R,R)-diethyl tartrate-diisopropoxide and its hydrolysis have been calculated. The mechanism for rapid ligand exchange with alkyl hydroperoxides involving the $Ti(O\text{-}i\text{-}Pr)_4$ precursor is examined to show how the active epoxidation catalyst is produced.

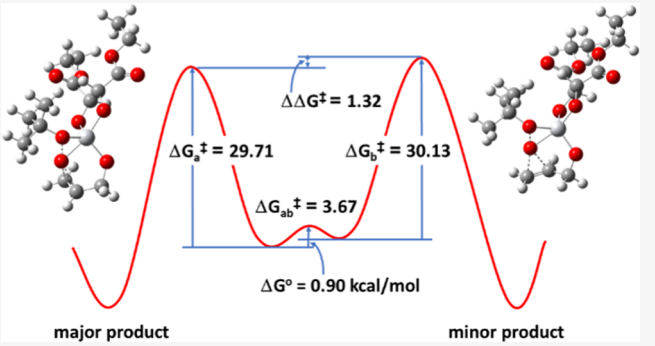

INTRODUCTION

Transition-metal-catalyzed epoxidations have been of considerable importance to the synthetic community for a number of years.[1,2] Introduction in 1980 of the titanium catalyst in the Sharpless reaction[3] presented an entirely new method for enantioselective epoxidation reactions. This series of transition-metal catalysts utilizing alkyl hydroperoxo intermediates provided one of the first general laboratory methods to synthesize enantiomerically pure epoxides. Although much is known about this widely employed epoxidation method, some of the mechanistic conundrums concerning what exactly is responsible for such high enantiomeric excesses remains a mechanistic challenge to this day. The Sharpless catalyst is based upon the ligand exchange of titanium(IV) isopropoxide ($Ti(O\text{-}i\text{-}Pr)_4$) with diethyl tartrate (DET) that produces the chiral reagent [$Ti(DET)(O\text{-}i\text{-}Pr)_2$], as exemplified in Figure 1.

Subsequently, this dimeric intermediate is thought to undergo further very rapid ligand exchange with alkyl hydroperoxides such as *tert*-butyl hydroperoxide (*tert*-BuOOH) and the allylic alcohol substrate (HOAllyl) to produce the "loaded catalyst".[4,5]

The oxidation of organic compounds can involve a wide variety of peroxides, and each of them can proceed with very different mechanistic motifs. The Ti(IV)-catalyzed epoxidation reaction proceeds in a very different manner from other alkene

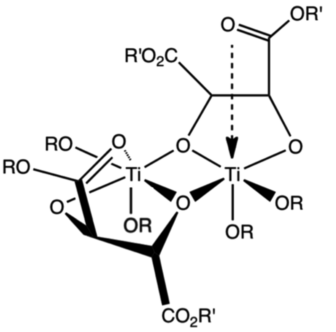

Figure 1. Proposed dimeric structure of $Ti(tartrate)(OR)_2$ in the Sharpless epoxidation reaction.

oxidation reactions as described below. We have recently provided a systematic study that compares the mechanism of oxygen atom transfer for several well-established oxidation

Received: September 25, 2021
Revised: November 22, 2021

reactions.[6] For example, in the peroxyacid epoxidation of an alkene, its OOH hydrogen is strongly hydrogen-bonded internally to the C═O oxygen, but in the TS, this hydrogen undergoes a 1,4-hydrogen shift almost immediately along the reaction coordinate in concert with its distal oxygen being transferred to the C═C bond (eq 1)

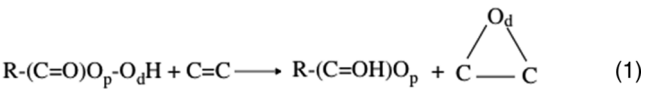

(1)

A somewhat related mechanism is involved when an alkyl hydrogen peroxide is involved in hydrocarbon oxidation (eq 2)

$$(\mathrm{R{-}O_p - O_d - H + H - C} \rightarrow [\mathrm{R{-}O_p \cdots H - O_d \cdots H \cdots C}] \rightarrow \mathrm{R - O_pH + H - O_d - C} \quad (2)$$

In this oxidation, the hydrogen of the hydroperoxide OOH group undergoes a 1,2-hydrogen shift to the proximal oxygen, and as noted above, it is the distal oxygen that is transferred to the substrate. We have referred to this 1,2-concerted hydrogen shift as a somersault-like rearrangement.[7] The first step in this overall oxidative process is abstraction of a hydrogen atom from the alkyl C−H group by the hydrogen-bonded hydroxyl radical ($HO^{\bullet}$) to produce a water molecule that remains hydrogen-bonded to the proximal oxygen. It is this positive H-bonding interaction ($R{-}O_p{\cdots}H{-}O_d$) of the transferring H atom to the proximal oxygen that tends to stabilize the TS and lowers the overall activation barrier. One salient feature of this oxidative process is that the abstracted hydrocarbon H atom remains with the hydrocarbon moiety in its newly formed hydroxyl group. Thus, the peroxide hydrogen atom is fully transposed to the hydroxyl group of the alcohol functional group derived from the initial hydroperoxide.[6] We have also suggested that these concepts can be extended to metastable metal hydroperoxides that also involves the rearrangement of the ground-state metal hydroperoxide to its inverted isomeric form with a hydroxyl radical hydrogen-bonded to the metal oxide (MO-OH → $MO^{\delta\bullet}{\cdots}HO^{\delta\bullet}$). We have introduced these mechanistic principles involving a somersault motion for iron hydroperoxides (FeO−OH → FeO···HO) in the Fenton oxidation.[8] This type of novel peroxide rearrangement can also be operating in enzymatic reactions that we have suggested for P450 model porphyrin iron(III) hydroperoxide [Por(SH)Fe-(III)−OOH−].[7] We have also suggested that this 1,2-hydrogen shift is operating in the oxidation step for flavin monooxygenases (FMO) and for the mechanism of the hydroxylation between L-Kyn and model FAD-hydroperoxide in the presence of KMO enzyme.[9]

Since the introduction of the Sharpless reaction in 1980,[3] there have been a great many experimental papers published on the mechanism of this reaction. However, there have been surprisingly few theoretical papers on an epoxidation reaction of this importance. In 1995, Wu and Lai[10] reported a rather comprehensive DFT study on the Sharpless epoxidation that included the dimeric catalyst with allyl alcohol (prop-2-en-ol) and *tert*-butyl hydroperoxide. However, the overall size of the catalyst system, at that time, precluded full geometry optimization and the basis set was limited to BYLP/3-21G. They also reported a TS for trihydroxytitanium hydroperoxide ($(HO)_3Ti(IV)OOH$) epoxidation of ethylene (BLYP/3-21G) and an activation energy of 10.7 kcal/mol (HW3/3-21G).[11] DFT studies by Root et al.[12] on the origin of the reactivity of titanium hydroperoxo catalysts in the epoxidation of ethylene were subsequently reported. Poblet et al.[13−15] have reported more recent DFT studies on the H_2O_2 epoxidation of ethylene catalyzed by Ti(IV)-containing polyoxometalates and defined the role of the metal and the coordination environment of the Ti(η^2-OOH) moiety.

The most recent study on the epoxidation of allyl alcohols with H_2O_2 was catalysis by a heterogeneous Ti-silicate intermediate, where the alcohol can be bonded to the Ti center and the H_2O_2 dissociates to form the nonligated reactive Ti(η^2-OOH) moiety.[2] Although these studies report many novel mechanistic features of alkene epoxidation with Ti-containing polyoxometalates, none of the above studies based upon H_2O_2 as the oxidative reagent can serve as a model for the Sharpless epoxidation. The most egregious omission in this series of H_2O_2-based Ti catalysts is the absence of the obligatory hindered alkyl hydroperoxide Ti ligand. In these H_2O_2-Ti(IV) catalytic systems, the rate-limiting η^2 O−O bond cleavage step involves migration of the hydroxy anion to the Ti center and this cannot play any steric role in the enantioselectivity of the resulting epoxide. For this reason, the peroxide of choice for the Sharpless epoxidation is *tert*-butyl hydroperoxide.[3]

The first and only TS for a Ti(IV)-catalyzed epoxidation using an alkyl hydroperoxide was reported in 2002. Adam and Jiang et al.[16] used DFT calculations (B3LYP/6-31+G(d,p)) to study the diastereoselective epoxidation of a series of methyl-substituted allylic alcohols. This DFT model study provided insight into how 1,3-steric repulsion and the electronic orbital interactions of a spiro-TS can influence the erythro/threo epoxide product ratio. However, in this series of bimolecular epoxidation reactions, the simplified $Ti(OH)_4/CH_3OOH$ was used as an oxidant model for Sharpless oxidant $Ti(O\text{-}i\text{-}Pr)_4$/*t*-BuOOH. We now report a series of TSs for the epoxidation of Ti-bound allyl alcohol where the Ti(IV) catalyst is composed of the bidentate(R,R)-(+)-diethyl tartrate chiral auxiliary and *tert*-butyl hydroperoxide that are the basis of the Sharpless epoxidation.

COMPUTATIONAL METHODS

The density functional theory (DFT) calculations were performed with Gaussian 16.[17] The minima and transition structures involving oxygen atom transfer presented in the figures and discussed in the text were fully optimized[18] using the M06-2X density functional[19] with the 6-311+G(d,p) basis set unless otherwise noted. We have found that the M06-2X functional provided very good O−O bond dissociation enthalpies, while the B3LYP functional[20,21] underestimates the energetics of the O−O bond cleavage.[22,23] The reactions involving the addition of H_2O to the Ti center and subsequent dimerization used the B3LYP/6-311+G(d,p) basis set. The allyl C−C bond rotational barriers for **TS-4ab** and **TS-5ab** were obtained using a potential energy scan with geometry optimizations at either 10 or 5° intervals to observe a maximum on the reaction coordinate followed by locating the transition state (TS) with a dihedral angle close to that maximum. Frequency calculations were carried out on all fully optimized structures at this same level to verify that they are either minima or first-order saddle points (TSs). Cartesian coordinates, total SCF energies, enthalpies at 298 K, and Gibbs free energies at 298 K are listed in the Supporting Information.

https://doi.org/10.1021/acs.jpca.1c08447
J. Phys. Chem. A XXXX, XXX, XXX−XXX

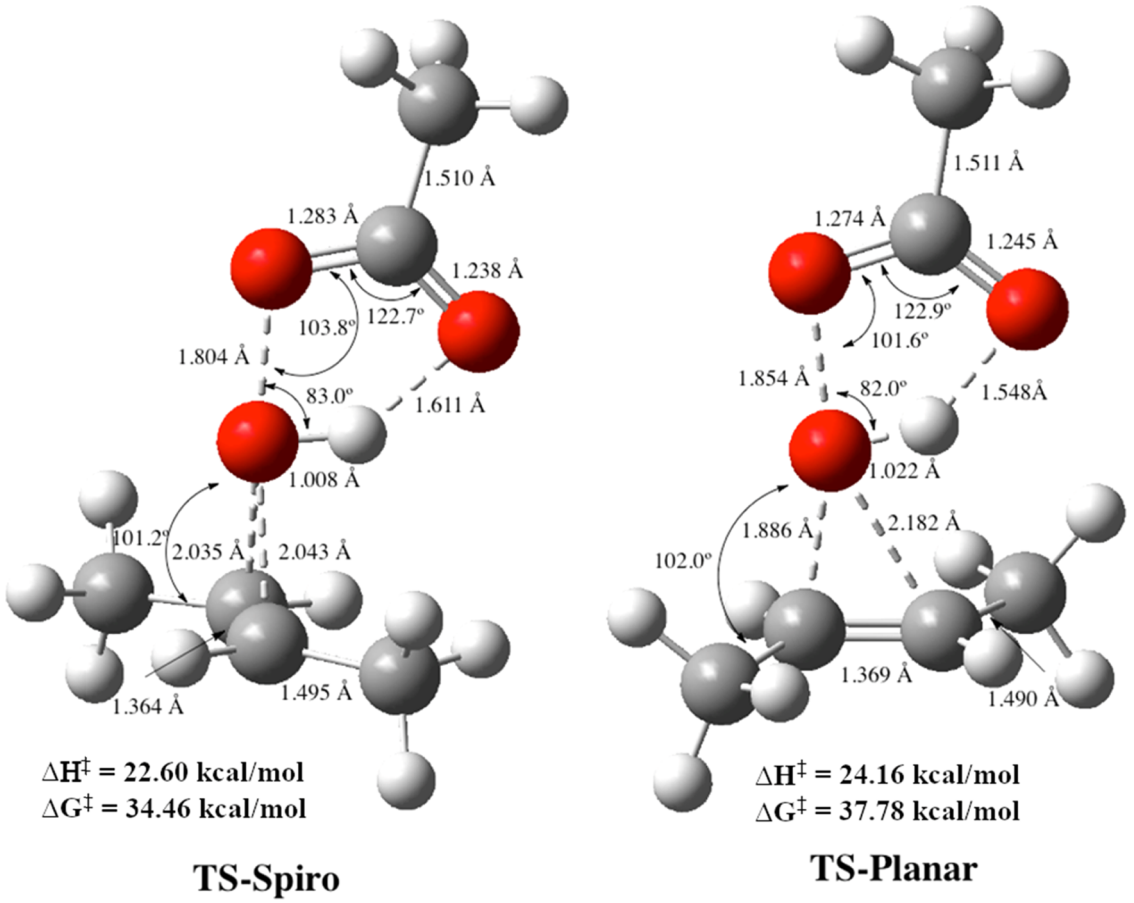

Figure 2. Spiro and planar transition structures for E-2-butene epoxidation with peroxyacetic acid.

Relative enthalpies and Gibbs free energies are given in the figures.

RESULTS AND DISCUSSION

We recently reported a revised study describing the O−O bond dissociation enthalpies (BDEs) for a series of peroxides of varying structures.[23] The finding that the M06-2X density functional provides O−O BDEs within 1−2 kcal/mol of the values obtained with the higher-level composite CBS-APNO method[23] prompted us to use the M06-2X functional in the current study. We have also recently shown that the M06-2X functional provides comparable accuracy on BDEs for the N−O bond.[24] Although the B3LYP density functional has provided reasonably good activation barriers in the past for such oxidative reactions, we have employed the M06-2X functional in this study to provide comparative activation energies since these reactions involve the O−O bond cleavage. This series of organic peroxide catalysts include a model Ti(IV) *tert*-butyl hydroperoxide, and we found that its O−O BDE was much higher than might have been anticipated. While the O−O BDE of a generic peroxide has now been ascribed a bond energy of ca. 45 kcal/mol,[23] we also reported that an O−O BDE approaches 60 kcal/mol (CBS-QB3) for a titanium peroxide ($(RO)_3TiO\text{-}OC(CH_3)_3$) that models the Sharpless catalyst. This prompted us to examine the activation energy for alkene epoxidation with this catalyst and how it compares with more classical organic peroxides such as a peroxyacid. In so doing, we have examined several of the more important individual mechanistic steps of the Sharpless epoxidation of allylic alcohols with a monomeric titanium catalyst. This allows us to examine these mechanistic nuances in more detail than would be possible on the dimeric catalyst that is much more computer-intensive.

Mechanism for Oxygen Atom Transfer with Ti(IV) Catalysis. It is generally thought that in alkene epoxidation the peroxide O−O bond should approach the center of the C═C π-bond in as close to a linear manner as possible in the oxygen transfer step. This point is best examined in a bimolecular reaction where there are no geometrical constraints on the approach of the peroxide O−O bond to the C═C π-bond. It has also been established that the epoxidation TS with a variety of oxidizing agents has a spiro orientation,[25,26] where the planes of the R−C═C−R π-bond and X−O−O (where X is the C of a peroxyacid or the Ti atom of the Ti(IV) catalyst) peroxide system are perpendicular to each other. In this geometrical approach, the incoming oxygen lone pair has the proper symmetry to interact with the π^* orbital of the alkene. The angle between the COC plane of the epoxide product being formed and the plane of the X−O−O group should approach 90° for a spiro-TS or near 0° for a planar TS. This idealized molecular approach is exemplified by examining the bimolecular epoxidation of E-2-butene with peroxyacetic acid (Figure 2).

In the **Spiro-TS**, the angle between the incoming O−O bond and the midpoint of the C═C bond is 179.4° for an unencumbered approach of the two interacting moieties. In addition, the angles between the C−O−O plane and the C═C−H and C−O−C planes of the developing epoxide are 90.3

https://doi.org/10.1021/acs.jpca.1c08447
J. Phys. Chem. A XXXX, XXX, XXX−XXX

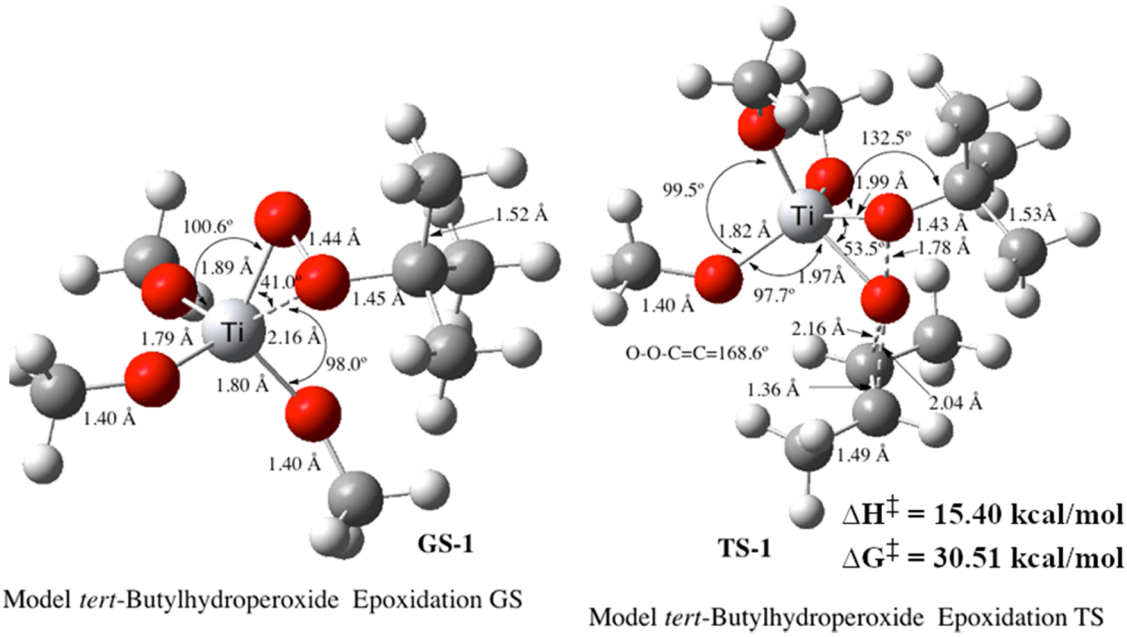

Figure 3. Epoxidation of E-2-butene with titanium(IV) *tert*-butyl hydroperoxide.

and 95.6°, respectively, supporting a nearly spiro orientation of the interacting frontier orbitals. The fact that the bond lengths of the two developing C−O bonds in the TS are essentially identical is what is expected for the spiro orientation. It is noted that the bulk of the peroxyacid is over one side of the E-2-butene C═C bond axis and that is largely responsible for that angular distortion. The overall geometry of the **Spiro-TS** is typical of those TSs reported previously,[26] with an O−O bond elongation to 1.804 Å. The calculated activation enthalpy, $\Delta H^{\ddagger}$ = 22.60 kcal/mol, was considerably greater than $\Delta H^{\ddagger}$ = 13.12 kcal/mol[6] for this epoxidation reaction with the B3LYP functional and the same 6-311+G(d,p) basis set. This difference in energy barriers is not too surprising because the B3LYP functional on average exhibits an O−O BDE that is ca. 11 kcal/mol lower than that with the M06-2X functional.[23]

In an effort to gain an appreciation for the magnitude of the electron lone-pair alkene π^* orbital interaction, we constrained the geometry of the two interacting reactants to be in a planar relationship throughout the oxygen transfer step (**Planar TS**; Figure 2). The computed enthalpy barrier for the planar TS ($\Delta H^{\ddagger}$ = 24.16 kcal/mol) is 1.56 kcal/mol greater than that of the spiro-TS. While other interactions may contribute, the energy difference in this relatively uncrowded case provides an estimate for how the π^* orbital interactions in the spiro orientation could influence the activation energy. The approach of the peroxyacid to the C═C bond in **TS-Planar** is quite asymmetrical, with the two developing C−O bonds being quite different (1.886 vs 2.182 Å). This constrained TS is a second-order saddle point (ν_i = 602.5*i* and ν_i = 43.3*i*). The smaller imaginary frequency corresponds to a rotation of the peroxyacid plane from planar toward a spiro orientation. Since the average single C−O BDE is generally assumed to be about 84 kcal/mol, the energetics of the asymmetrical C−O bond formation in the TS can markedly affect the activation energy and consequently this is a factor that must be considered in assessing differences in the $\Delta G^{\ddagger}$ for evaluating the enantiomeric excess in a chiral epoxidation reaction. An estimate of the effect that asymmetric C−O bond development can have on the activation barrier can be gleaned from elongation of the C−O bond in dimethyl ether by 0.1 Å, where the overall increase in energy is 2.67 kcal/mol. Thus, the asymmetric C−O bond formation in the TS can compete with π^* orbital electronic interactions to determine the enantiomeric selectivity.

We now extend these fundamental concepts for the oxygen transfer to include a bimolecular epoxidation catalyzed by a Ti(IV) peroxide. The simplest model titanium(IV) hydroperoxo catalyst that we can employ with the commonly used *tert*-butyl hydroperoxide oxidant is the catalyst $(MeO)_3TiO_p$-$O_dC(CH_3)_3$ presented in Figure 3. The O−O bond is bound to the Ti center in the well-established bidentate η^2 manner, with the proximal Ti−O_p bond distance (1.89 Å) and the secondary distal η^2 Ti−O_d bond distance (2.16 Å) being somewhat longer.

The epoxidation of E-2-butene (Figure 3; **TS-1**) with this Ti metal-catalyzed oxidant has a relatively low activation barrier ($\Delta H^{\ddagger}$ = 15.40 kcal/mol). The most favorable orientation for the O atom transfer is a near-linear approach of the O−O bond to the center of the alkene C═C bond (calculated C═C midpoint-O−O angle = 176.2°). Steric interactions in **TS-1** can cause it to deviate from a pure spiro orientation. The angles between the OOTi plane and the C═C−H and C−O−C planes of the developing epoxide are 84.8 and 133.4°, respectively, in **TS-1**, suggesting a considerable deviation from the pure spiro orientation seen above in the above oxidation with peroxyacid, **Spiro-TS**. Nevertheless, the two developing C−O bonds have similar lengths, 2.04 and 2.16 Å. The O−O bond is elongated from 1.44 to 1.78 Å in the TS, and the two Ti−O bond lengths are now very close as the distal *tert*-butoxide is involved in a 1,3-migration to the Ti center accompanying the transfer of the proximal oxygen to complete formation of the 3-membered epoxide ring (eq 3)

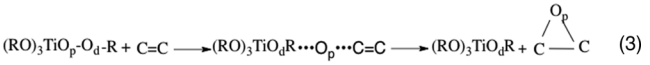

(3)

We can also provide a rationale for the relatively low calculated energy barrier for Ti(IV) catalyst epoxidation ($\Delta H^{\ddagger}$ = 15.40 kcal/mol) despite the high Ti−O−O bond dissociation

https://doi.org/10.1021/acs.jpca.1c08447
J. Phys. Chem. A XXXX, XXX, XXX−XXX

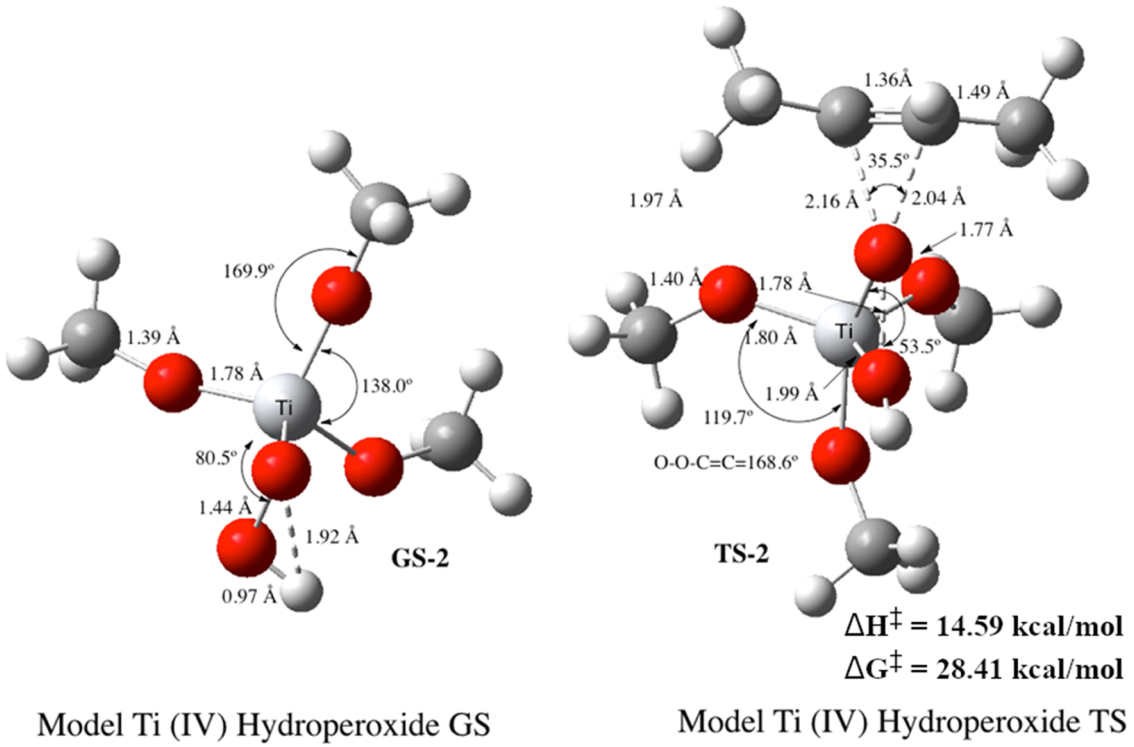

Figure 4. Epoxidation of E-2-butene with titanium(IV) hydroperoxide.

enthalpy for this Ti-bound peroxide (60 kcal/mol).[23] The O−O bond dissociation involves breaking both the O−O bond and secondary η^2 Ti−O bond. In contrast, the rate-limiting oxygen transfer step involves cleavage of the primary Ti−O bond in concert with a shortening of the secondary η^2 Ti−O bond attending the 1,3-OC$(CH_3)_3$ ligand migration, thereby reducing the activation barrier. It was recognized very early in the development of the Sharpless reaction that in the TS the OOR ligand is bound covalently to the Ti atom, thereby activating the oxygen proximal to the metal to transfer to the substrate.[27] In the present study, we simply describe this molecular motion as a 1,3-rearrangement of the *tert*-butyl group with the oxygen proximal to the Ti transferred to the alkene substrate. This provides a comparison with the three different oxidation reactions presented in eqs 1−3 and makes their subtle mechanistic differences more discernible.

Comparison of this Ti-catalyzed oxidation (**TS-1**) with the epoxidation of E-2-butene with peroxyacetic acid ($\Delta H^{\ddagger}$ = 22.60 kcal/mol) with the same level of theory (M06-2X/6-311+G(d,p)) suggests that this type of titanium alkyl peroxo catalyst is much more reactive than a peroxyacid ($\Delta\Delta H^{\ddagger}$ = 7.20 kcal/mol). The peroxyacid **Spiro-TS** when optimized without geometry constraints has a nearly pure spiro orientation since the OOC plane of the peroxyacid is nearly perpendicular to the C═CH and C−O−C planes. When the peroxyacetic acid moiety is constrained to be planar with respect to the C═C bond axis that TS is 1.56 kcal/mol higher in energy than the spiro-TS. Thus, it is easily recognized that any deviation from a pure spiro orientation as a consequence of steric interactions can increase the activation energy for epoxidation. In the Sharpless epoxidation, it is the orientation or approach of the electrophilic oxygen imposed by the dihedral angle of the allylic alcohol that controls the requisite C═C stereoface that receives the oxygen and determines the stereoselectivity of the resulting epoxide product.

We also made the comparison of the calculated activation energy for the above Ti metal-catalyzed oxidant with the M06-2X functional (**TS-1**) with that calculated with the B3LYP functional and observed a comparable barrier ($\Delta H^{\ddagger}$ = 16.66 kcal/mol, $\Delta\Delta H^{\ddagger}$ = 1.26 kcal/mol) with the same basis set. In general, over the years, the B3LYP functional has provided reasonable activation barriers in agreement with experimental data for a wide variety of oxidation reactions.[26,28] Why this Ti(IV)-catalyzed epoxidation has a relatively close activation barrier while that for peroxyacid epoxidation (**Spiro-TS**) with the B3LYP versus the M06-2X functional has a $\Delta\Delta H^{\ddagger}$ = 9.48 kcal/mol continues to remain an enigma. The O−O BDEs calculated with the B3LYP functional on average exhibit a BDE that is ca. 11 kcal/mol lower than that with the M06-2X functional[23] despite the fact that in the rate-limiting epoxidation TS, the O−O bond cleavage is involved in both cases.

To provide a comparison with the many reported metal-catalyzed[1,2] oxidation reactions using the hydroperoxo ligand derived from H_2O_2, we also carried out the epoxidation of E-2-butene with the hydroperoxo (OOH) catalyst (Figure 4). The activation barrier for **TS-2** ($\Delta H^{\ddagger}$ = 14.59 kcal/mol) is nearly the same as that with the above *tert*-butoxide ligand (**TS-1**, $\Delta H^{\ddagger}$ = 15.40 kcal/mol) despite the fact that the O−O BDE in H_2O_2 is 5−6 kcal/mol higher than that in *tert*-butyl alcohol.[23] We also observe an essentially linear approach (176.3°) of the proximal oxygen to the center of the C═C π-bond, with O−O−C bond angles identical to those reported above (**TS-1**) and also with the same degree of O−O bond elongation (R_{O-O} = 1.78 Å) in the TS.

As anticipated, we observe a 1,3-migration of the O_dH group distal to the titanium metal center in concert with the transfer of the proximal (O_p) oxygen to the C═C π-bond, as indicated in eq 3. The angles of the OOTi plane with the C═C−H and C−O−C planes of the developing epoxide in **TS-2** (88.1 and

https://doi.org/10.1021/acs.jpca.1c08447
J. Phys. Chem. A XXXX, XXX, XXX−XXX

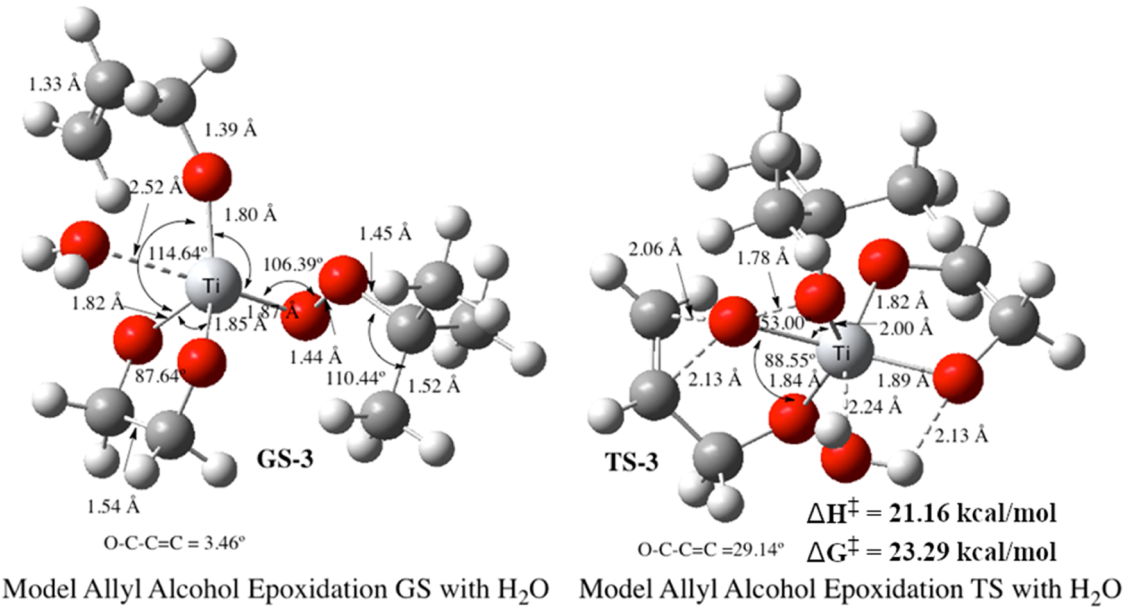

Figure 5. Epoxidation of E-2-butene with titanium(IV) *tert*-butyl hydroperoxide with a bound H_2O molecule.

130.6°, respectively) are nearly the same as for the alkyl peroxo ligand (**TS-1**, 84.8 and 133.4°).

In the present study, we are dealing with flexible and low-coordinated relatively unhindered TSs as the calculated structures of **TS-1** and **TS-2**, and in such cases, we always anticipate that it is the proximal or α-oxygen that is transferred. In contrast, DFT calculations have suggested that with rigid and highly hindered Ti centers it is the distal or β-oxygen that is transferred in the epoxidation reaction and this can even lead to lower activation barriers.[29] It has also been shown that the formation of these titanium hydroperoxo intermediates is greatly facilitated by the presence of protic solvent molecules in the immediate coordination sphere.[29] In this case, protonation of the H_2O_2 moiety itself activates the O−O bond and is largely responsible for lowering the activation barrier.[14]

Hexacoordinate versus Pentacoordinate Ti Center. It has been well established that the Ti atom in the dimeric Sharpless catalyst has a hexacoordinate environment.[3,4] To achieve this, we simply add a H_2O molecule to the Ti center of our monomeric model Ti(IV) *tert*-butyl hydroperoxide catalyst to model the bridging oxygen in the dimeric structure, as suggested by Wu[10] in his theoretical study on the Sharpless catalyst. This model catalytic system includes an allyl alcohol that is tethered to the Ti center and hence involves an intramolecular oxygen atom transfer. We included an ethylene glycol moiety to model the chiral bidentate tartrate auxiliary in the Sharpless catalyst (Figure 5).

In ground state **GS-3**, the primary Ti−O bond distance is 1.87 Å, while the secondary η^2-Ti···O bond distance is greater at 2.12 Å. The O−C−C═C dihedral angle (3.46°) of the allyl alcohol in **GS-3** is of great importance in these studies because it is this C−C rotational angle that presents the desired C═C stereoface to the transferring oxygen in the TS. This orientation, with respect to the transferring oxygen atom, determines the chirality of the epoxide when dealing with optically active substrates. It is also noted that the angles of the OOTi plane with the C═C−H and C−O−C planes of the developing epoxide in **TS-2** (94.5 and 82.6°, respectively) are close to spiro as is the approach of the O−O bond to the C═C midpoint (168.7°). The O−C−C═C dihedral angle in **TS-3** is 29.4°, and, due to the geometrical constraints, the approach of the transferring oxygen is slightly asymmetric with C−O bond distances of 2.06 and 2.13 Å in the developing epoxide in accord with a small distortion from a pure spiro orientation. In **TS-3**, both of the Ti−O bonds are at 2.00 Å as the proximal oxygen is transferred to the C═C bond and the migrating $OC(CH_3)_3$ ligand is bound (2.00 Å) to the central Ti atom.

In **TS-3**, a H_2O was added to achieve a hexacoordinate titanium peroxo so that the monomer environment is equivalent to that in the dimeric Sharpless catalyst. We next omitted the water ligand from the Ti(IV) center and repeated the above epoxidation reaction (Figures 6 and 7). We located two ground-state conformers that expose different faces of the C═C bond to the transferring oxygen atom in the TS.

In ground state **GS-4a**, the C═C and C−O bonds in the allyl alcohol moiety are essentially eclipsed with an O−C−C═C dihedral angle of 0.73°. This conformer is slightly lower in energy (ΔG = 1.89 kcal/mol) than **GS-4b** that presents the opposite C═C face and has a dihedral angle of 236.9° (Figure 6). The C−C bond rotation for interconversion of these two equilibrating conformers exhibited a maximum at a dihedral angle of 56.1° in **TS-4ab** and has a relatively low activation barrier ($\Delta G^{\ddagger}$ = 4.11 kcal/mol). However, it should be noted that the energy profile of the dihedral angle can be altered by 3−4 kcal/mol due to substituents on the allyl alcohol such as a methyl group.[16]

With oxygen atom transfer to **GS-4a**, we observe an increase in the O−C−C═C dihedral angle of 33.9°. The transition state for epoxidation reaction (**TS-4a**; Figure 7) has an activation barrier of $\Delta G^{\ddagger}$ = 30.83 kcal/mol. This represents a marked increase in epoxidation activation energy ($\Delta\Delta G^{\ddagger}$ = 7.54 kcal/mol) with the pentacoordinate Ti(IV) catalyst relative to hexacoordinate **TS-3**. The approach of the O−O bond to the C═C midpoint is somewhat off from linear (162.2°) and has a nearly spiro orientation (79.7 and 95.0° for the angles between the OOTi plane and the C═C−H and C−

https://doi.org/10.1021/acs.jpca.1c08447
J. Phys. Chem. A XXXX, XXX, XXX−XXX

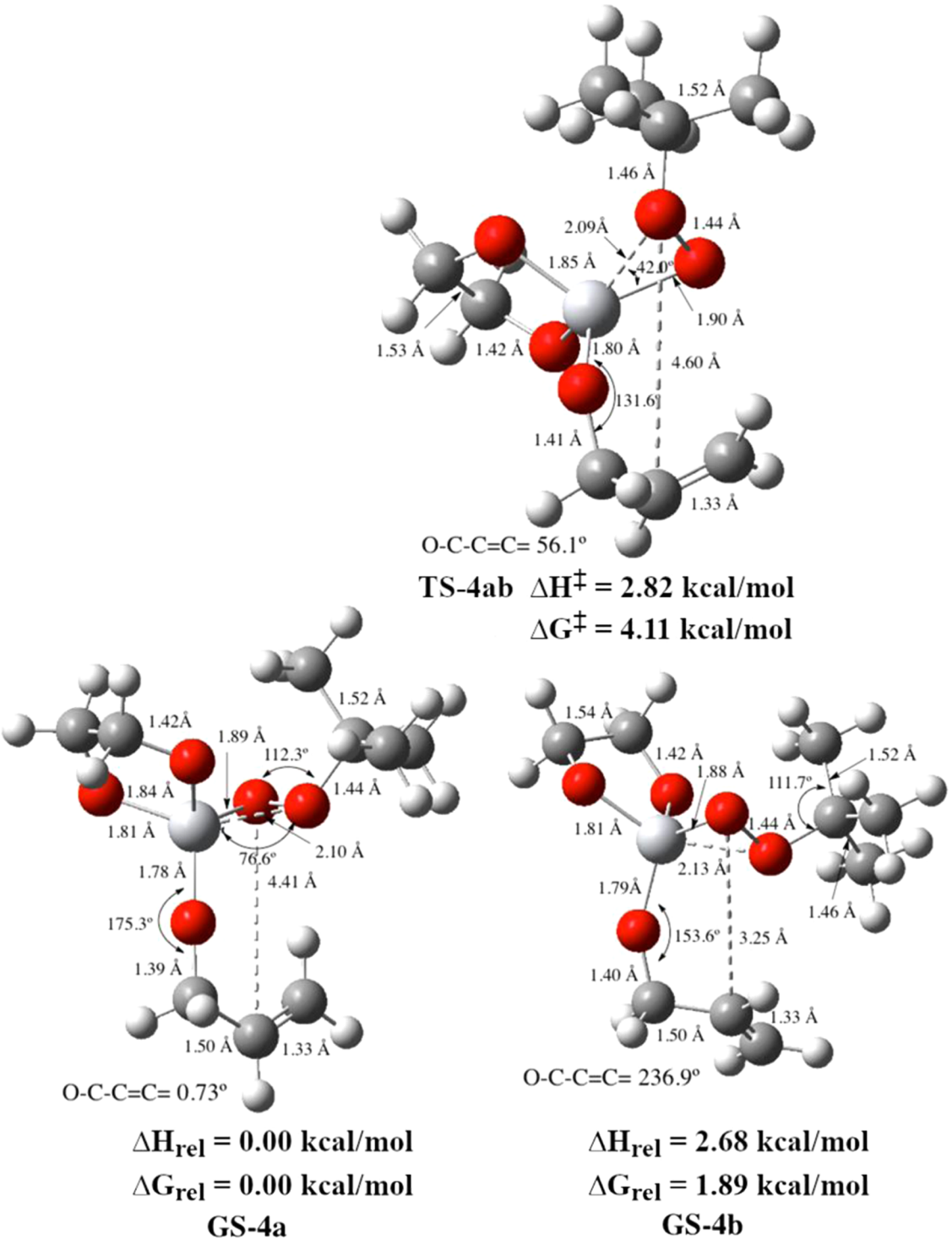

Figure 6. Ground states **4a** and **4b** and the transition state **TS-4ab** for rotation about the C−C bond in the allyl alcohol.

O−C planes). Elongation of the O−O bond to 1.78 Å in **TS-4a** is accompanied by Ti−O bond distance changes resulting in two nearly equivalent Ti−O bonds (1.94 and 1.98 Å) and two developing C−O bonds of the epoxide (2.08 and 2.12 Å).

With epoxidation of the other conformer (**GS-4b**), the approach of the peroxide moiety is about the same as that in **TS-4a** (166.6°) but the transition state has a nearly planar orientation (106.9 and 9.6° for the angles between the OOTi plane and the C═C−H and C−O−C planes). The O−C−C═C dihedral angle, 245.3°, is only a little different from that in **GS-4b** (236.9). The geometric features of the two TSs are quite similar with developing C−O bonds in the **TS-4b** of 2.03 and 2.13 Å. The activation barrier is nearly the same as in **TS-4a** ($\Delta\Delta G^{\ddagger}$ = 0.24 kcal/mol) but it must be recalled that the **GS-4b** is 1.89 kcal/mol higher in energy. To understand the relative rates for these two epoxidation reactions, we need to consider the Curtin−Hammett principle.[30]

In each of these epoxidation reactions, involving an allyl alcohol, where conformers can interconvert rapidly, the product ratio can depend both upon their difference in energy

https://doi.org/10.1021/acs.jpca.1c08447
J. Phys. Chem. A XXXX, XXX, XXX−XXX

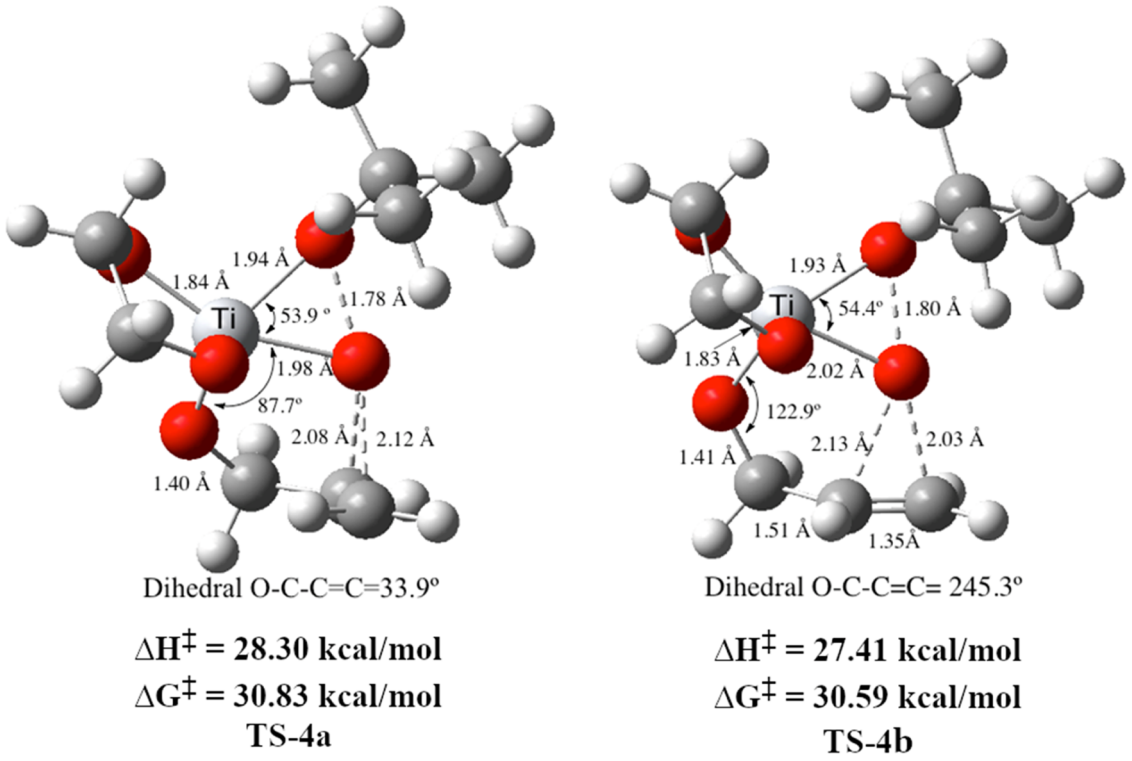

Figure 7. Transition states for the Ti(IV)-catalyzed epoxidation of allyl alcohol.

and the energy barriers for each of the rapidly equilibrating isomers that produce a different epoxide product. With simple substituted allyl alcohols, the C−C rotational activation barrier is typically much lower than that for epoxidation and the product distribution (enantioselectivity) reflects the difference in Gibbs free energy between the two rate-limiting transition states. As evidenced in the Curtin−Hammett plot (Figure 8),

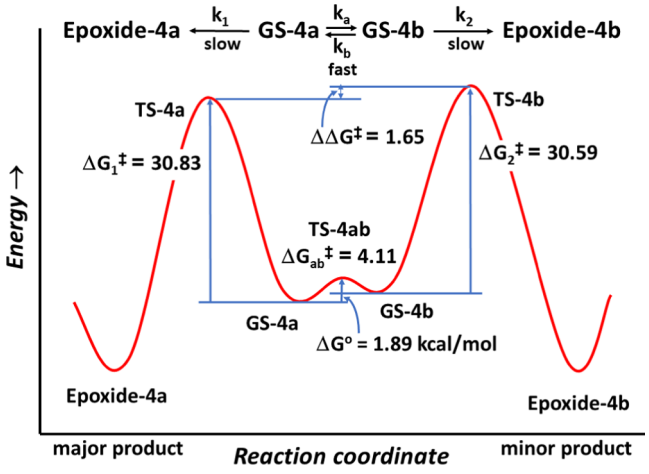

Figure 8. Curtin−Hammett plot for the Ti(IV)-catalyzed epoxidation of allyl alcohol (Δ*G* in kcal/mol).

the Gibbs free-energy difference between the two GS conformers (ΔG = 1.89 kcal/mol) is very small and the Gibbs free energy of activation for equilibration between these two conformers is $\Delta G^{\ddagger}$ = 4.11 kcal/mol with respect to the lower-energy minimum **GS-4a**. When we compare the Gibbs free energies of activation for epoxidation, we find that they are nearly equal, with $\Delta G^{\ddagger}$ = 30.83 kcal/mol for **GS-4a** → **TS-4a** and 30.59 kcal/mol for **GS-4b** → **TS-4b**. However, the ratio of products depends on the Gibbs free-energy difference of the transition states, $\Delta\Delta G^{\ddagger}$ = 1.65 kcal/mol, in favor of the **Epoxide-4a** product.

Since the activation barriers are so close to each other, the two differing O−C−C═C dihedral angles in the TS cannot play a major role in this simple model case in determining the epoxidation barrier. It is this conformational change in the dihedral O−C−C═C angles in the allylic alcohol that was presumed to be largely responsible for the high enantiomeric selectivity in the Sharpless epoxidation reaction. The O−O bond alignment is in a spiro orientation in **TS-4a**, and the O−C−C═C dihedral angle is 33.9° in the TS with the lowest energy.

In the epoxidation TS, the 1,3-migration of the distal oxygen of the *tert*-butoxide results in a $OC(CH_3)_3$ ligand strongly bound to the titanium center in **Epoxide-4a** (Ti−O_d = 1.80 Å). The nature of the 1,3-rearrangement of the *tert*-butoxide ligand to the Ti atom is quite evident from the IRC analysis in Figure 9. In **GS-4**, the secondary Ti−O η^2 bond is 2.12 Å, and as the migration proceeds, this bonding distance decreases to 1.87 Å in **TS-4a** and the bonding distance of the Ti-$OC(CH_3)_3$ is further reduced to 1.80 Å in product **Epoxide-4a** (Figure 8). In **GS-4**, the O−O bond distance is 1.44 Å, whereas in **TS-4a**, this distance is 1.78 Å and at point 10 of the IRC (Figure 9; 66% of the energy decreases from **TS-4a** to **Epoxide-4a**), the O−O bond distance has increased to 2.22 Å as the O−O−Ti angle contracts and the $(CH_3)_3C$−O fragment decreases its bonding distance to the Ti atom from 2.12 to 1.87 Å. At point 20 of the IRC (92% of the energy decrease from **TS-4a** to **Epoxide-4a**), the Ti−O−$C(CH_3)_3$ bond is fully formed (1.80 Å). It is also evident that the epoxide oxygen is bound to the Ti center in the product (**Epoxide-4a**) with a bond distance of

https://doi.org/10.1021/acs.jpca.1c08447
J. Phys. Chem. A XXXX, XXX, XXX−XXX

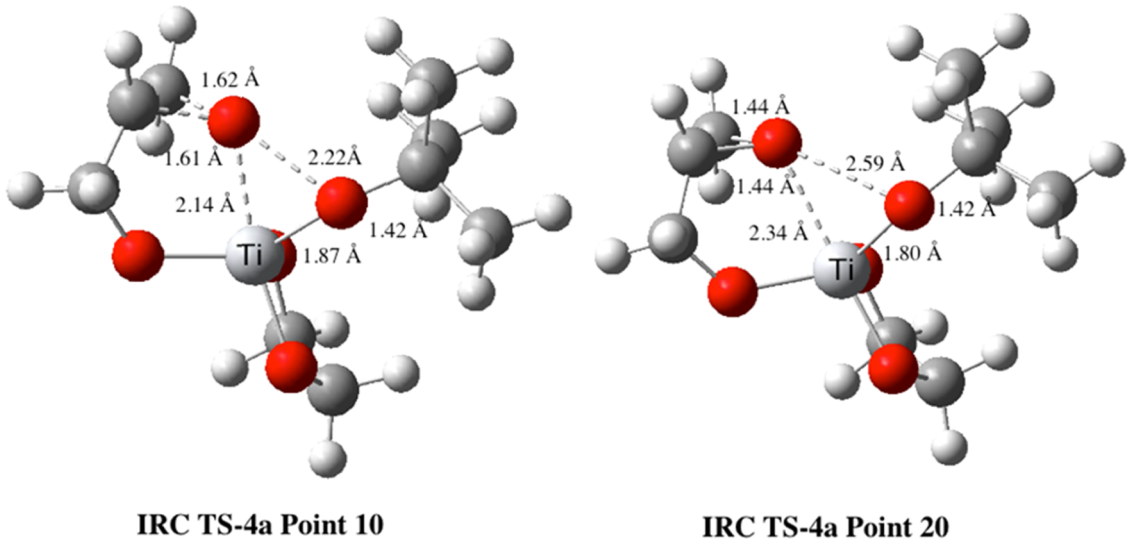

Figure 9. IRC for **TS-4a** in Figure 7.

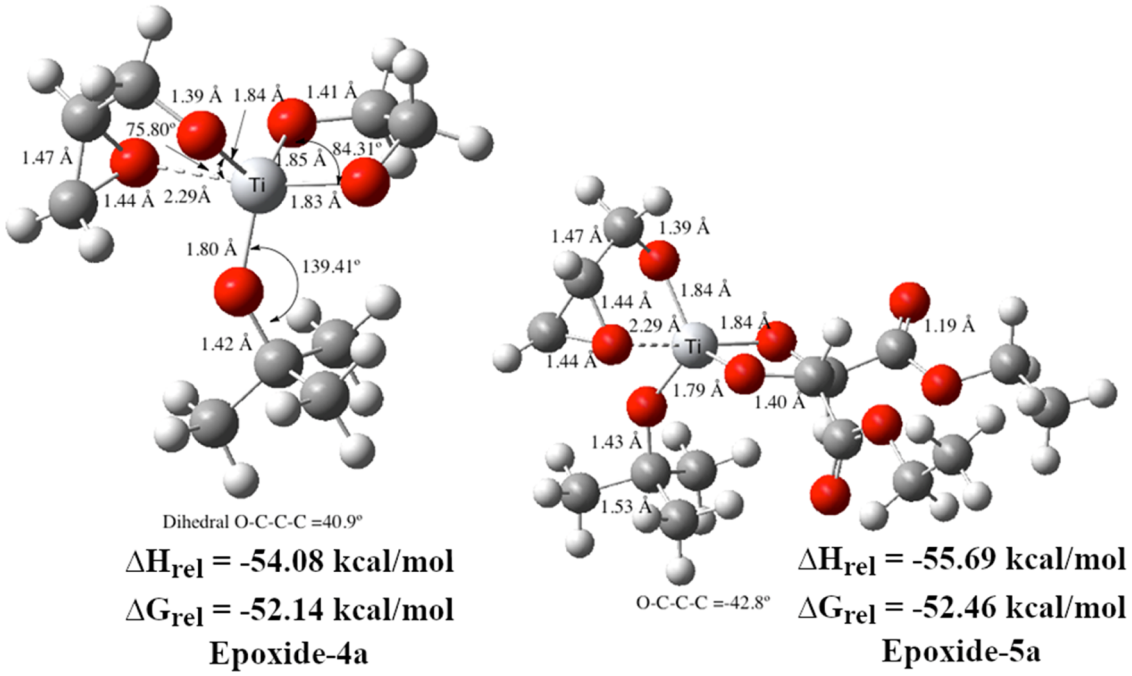

Figure 10. Products of epoxidation of **GS-4a** and **GS-5a** that contain the (R,R)-(+)-diethyl tartrate chiral auxiliary.

2.29 Å and that bond is essentially formed at point 20 of the IRC analysis.

As the oxygen being transferred is directed to the C═C bond, there should be only a minor change in the O−C−C═C dihedral angle. Indeed, the dihedral angles in the **TS-4a** and **Epoxide-4a** (Figure 10) are relatively close (33.90° vs 40.90°). The overall change in Gibbs free energy for product formation is $\Delta G = -52.14$ kcal/mol. It is also noteworthy that the epoxide oxygen forms a strong intramolecular secondary bond to the Ti center with a Ti−O distance of 2.29 Å. To estimate the strength of this intramolecular Ti−O bond, the OC−CC dihedral angle in **Epoxide-4a** was constrained to 180°, so that the epoxide oxygen is rotated away from the Ti atom and the Ti−O distance in the product was 4.73 Å. The energy of this constrained epoxide increased by 12 kcal/mol, suggesting that the relatively strong intramolecular Ti−O bond in the product contributes to its overall stability. This secondary bonding interaction could possibly help to lower the overall activation energy. It is also well known that epoxy alcohols are not stable under typical reaction conditions. The ring opening of the epoxide ring is activated by alcohols present in the reaction mixture to afford diols as a known byproduct that also can be accelerated by the presence of Lewis acids such as Ti(IV) alkoxides.[31]

The fact that an increase in activation energy attended the omission of a water molecule in the coordination sphere is consistent with the fact that a hexacoordinate environment is favored in the dimeric Sharpless catalyst.[4,32] However, it has been well established that the presence of water contributes not only to a lowering of the reaction rate but also to the enantioselectivity by interacting both reversibly and irreversibly with the dimeric catalyst.[33] In fact, just a single equivalent of

https://doi.org/10.1021/acs.jpca.1c08447
J. Phys. Chem. A XXXX, XXX, XXX−XXX

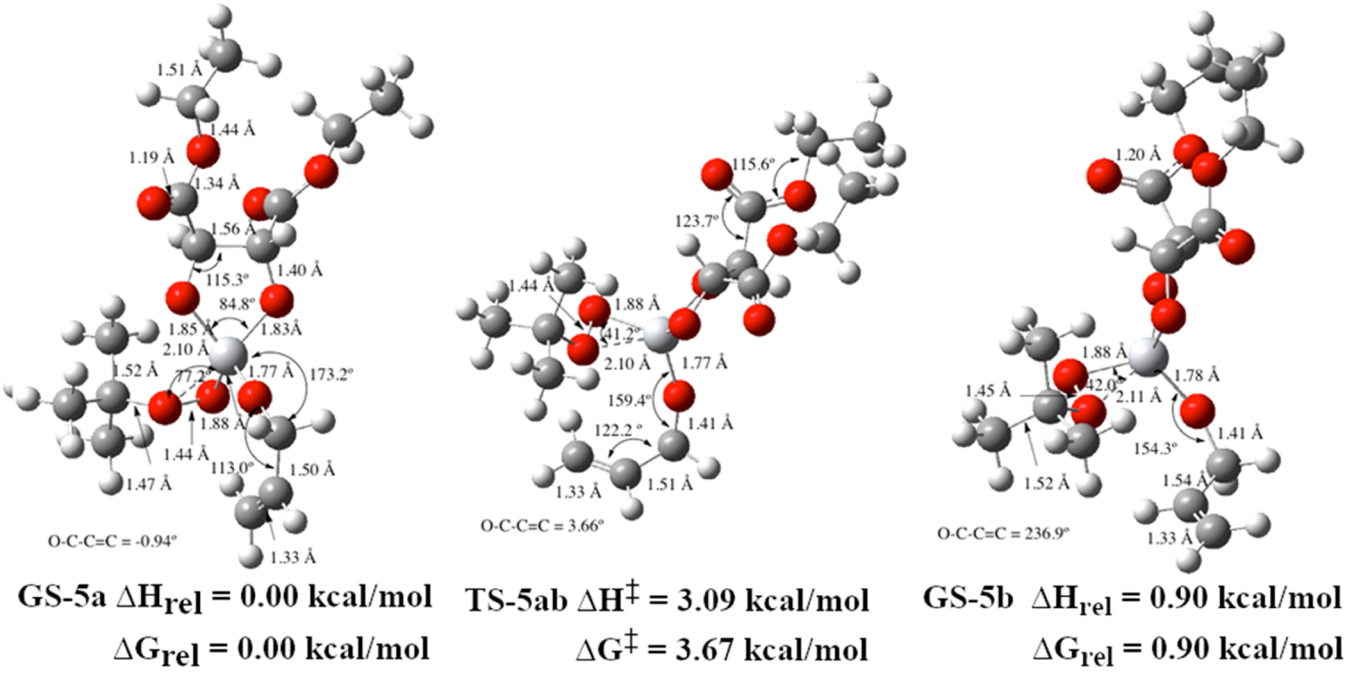

Figure 11. Equilibration of **GS-5a** and **GS-5b** with titanium(IV) *tert*-butyl hydroperoxide with the (R,R)-(+)-diethyl tartrate chiral auxiliary.

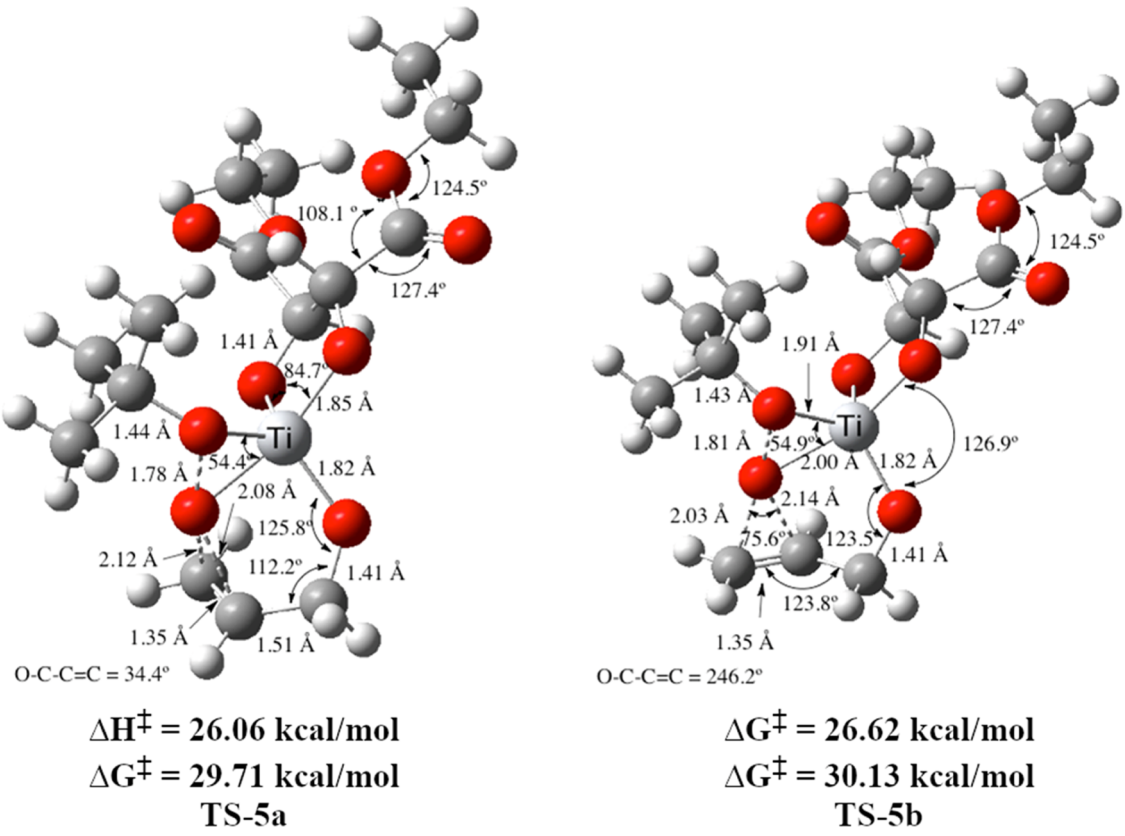

Figure 12. Epoxidation of allyl alcohol with titanium(IV) *tert*-butyl hydroperoxide with the (R,R)-(+)-diethyl tartrate chiral auxiliary.

water can destroy the catalyst. This problem was ameliorated by the presence of 3 or 4 A of molecular sieves to remove water, thereby effectively regenerating the catalyst.

Ti(IV)-Catalyzed Epoxidation with Bidentate (+)-(R,R) Diethyl Tartrate. In this model calculation for Ti(IV)-catalyzed epoxidation, we have used the monomeric Ti catalyst with allyl alcohol and the bidentate (+)-(R,R) diethyl tartrate chiral auxiliary with the *tert*-butoxide ligand (Figures 11 and 12). The lower-energy ground state (**GS-5a**) has the C═C eclipsed with the alcohol C−O bond with an O−C−C═C dihedral angle of 0.94°. The O−O bond distance in this conformer is 1.44 Å, and the primary Ti−O bond distance is characteristically shorter (1.88 Å) than the secondary η^2 Ti−O bond (2.10 Å). The bidentate tartrate diol oxygens comprising

https://doi.org/10.1021/acs.jpca.1c08447
J. Phys. Chem. A XXXX, XXX, XXX−XXX

the 5-membered ring have an O−Ti−O bond angle of 84.8°. The two C═O groups of the tartrate moiety are juxtaposed anti to one another with an O═C−C═O dihedral angle of 153°. The second conformer, **GS-5b**, has an O−C−C═C dihedral angle of 236.9° and is 0.90 kcal/mol higher in energy. As anticipated, the two ground-state conformers are rapidly equilibrating with an activation barrier of 3.67 kcal/mol (**TS-5ab**). Rotation of the O−C−C═C dihedral angle exhibited a maximum at 64.8° for **TS-5ab** in Figure 11.

The next objective is to locate the respective TSs for oxygen atom transfer to these two ground-state conformers. The approach of the O−O bond to the C═C bond center (162.2°) and the angles between the OOTi plane and the C═C−H and C−O−C planes (79.6 and 94.9°) are essentially the same as those in **TS-4a** (79.7 and 95.0°). In **TS-5a**, the O−C−C═C dihedral angle has increased to 34.4° relative to its ground state (0.94°) and has $\Delta G^{\ddagger}$ = 29.71 kcal/mol (Figure 12). The O−O bond in the TS has elongated from 1.44 to 1.78 Å, and the transferring oxygen atom forms nearly equal C−O bonds in the TS (2.08 and 2.12 Å). Like **TS-4a**, the structure of **TS-5a** is indicative of a spiro approach.

TS-5b has an O−C−C═C dihedral angle of 246.2° and has a barrier that is slightly higher than that of **TS-5a** ($\Delta\Delta G^{\ddagger}$ = 0.42 kcal/mol). The relevance of the O−C−C═C dihedral angles to produce face selectivity is quite evident in Figure 12, where the C═C bond is directed outwardly with a CH_2−C═C bond angle of 123.8°. Although the O−O bond approach angle (166.6°) and the C═CH/TiOO angle (107.3°) in **TS-5b** show a considerable deviation from ideal values, the developing epoxide C−O−C plane and the TiOO plane are nearly aligned (9.8°). If one looks down the O−O bond axis, **TS-5a** resembles a spiro-TS, while **TS-5b** approximates a planar approach. The near-planar orientation is a consequence of the strain that the O−C−C═C dihedral angle imposes on the developing C−O bonds in the TS.

Since the rate of interconversion between conformers **GS-5a** and **GS-5b** is very rapid and much greater than the rates of epoxidation, the Curtin−Hammett principle[30] applies, as noted above. In the present case, where both reactants are very close in energy, then the product ratio will depend only on the Gibbs free-energy difference of the transition states leading to the respective epoxide product. As evidenced in Figure 13, the Gibbs free-energy difference between the two GS conformers is very small (ΔG = 0.90 kcal/mol) and the Gibbs free energy of activation for equilibration between these two conformers is $\Delta G^{\ddagger}$ = 3.67 kcal/mol with respect to the lower-energy minimum **GS-5a**. When we compare the Gibbs free energies of activation for epoxidation, we observe that **GS-5a** → **TS-5a** ($\Delta G^{\ddagger}$ = 29.71 kcal/mol) differs from **GS-5b** → **TS-5b** ($\Delta G^{\ddagger}$ = 30.13 kcal/mol) by only 0.42 kcal/mol. However, the Gibbs free energy of the two transition states differs by 1.32 kcal/mol in favor of the spiro-TS-**5a** and **Epoxide-5a**. These data seem to support the concept that the origin of the enantiomeric excesses in the Sharpless epoxidation is a consequence of steric interactions that can affect subtle changes in geometry that can alter the electronic interactions in the TS.

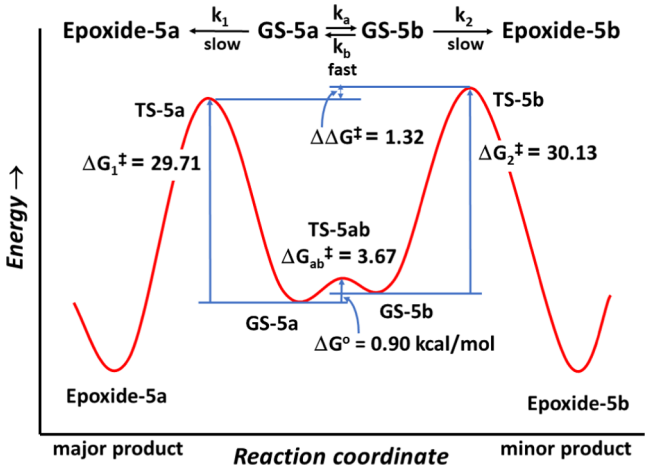

Figure 13. Curtin−Hammet plot for allyl alcohol with titanium(IV) *tert*-butyl hydroperoxide with the (R,R)-(+)-diethyl tartrate chiral auxiliary (ΔG in kcal/mol).

Dimerization of the Ti Catalyst. It has been well established[4] that the active catalyst in the Sharpless epoxidation is formed by ligand exchange in the dimeric form (Figure 1) of the titanium(IV) isopropoxide catalyst ($Ti(O\text{-}i\text{-}Pr)_4$). However, recent spectroscopy data have suggested that another asymmetric dimeric structure could exist that has two tartrates coordinated to a single Ti atom.[33] The structures used in that study have the less hindered methyl groups instead of the ethyl and isopropyl groups on the Sharpless catalyst and perhaps this presents a lesser steric problem. There have also been X-ray studies[32] and NMR data[4] that provide strong support for the proposed Sharpless dimer as the active catalyst.

One of the more notable features of the Sharpless epoxidation sequence is that the chirality of the product of epoxidation can be reliably predicted with a simple mnemonic.[3] If the (+)-diethyl tartrate is used, the *Re* face is attacked, preferentially leading to relatively high enantioselectivity in the manner described to produce the epoxide with the (S,S)-absolute configuration from a substituted C═C. However, upon inspection of monomeric catalyst **GS-5** (Figure 11), it is immediately obvious that the two chiral centers are too far removed from the active reaction site to have any influence upon the enantiomeric selection of the epoxide product. Even though the current study is restricted to a monomeric catalyst, we can still use these data to assist in our future calculations on the dimeric form of the catalyst. These data tend to support the idea that the dimeric form is essential to create sufficient steric congestion to result in a chiral epoxide. This is especially true since we observe a substantial increase in activation energy ($\Delta\Delta G^{\ddagger}$ = 7.54 kcal/mol) when we change from a hexacoordinate Ti environment, which is present in the dimeric form, to a pentacoordinate catalyst with the omission of a H_2O molecule binding to the Ti atom (Figures 6 and 7).

This prompted us to examine the dimerization energy of the pentacoordinate Ti(IV)-(R,R)-diethyl tartrate-diisopropoxide monomer (Figure 14). It is immediately obvious that the steric hindrance is increased surrounding any potential reaction site for epoxidation as described in the Sharpless reaction. The dimeric form $[Ti(DET)(O\text{-}i\text{-}Pr)_2]_2$ has a bridged arrangement of the tartrate bidentate ligand. One of the diol oxygens is directly bonded to the Ti center with a distance of 1.88 Å, whereas the oxygens bridging between the two Ti atoms have longer bond distances (R_{Ti-O} = 2.10, 2.04 Å). The distance between the two Ti atoms in this 4-membered ring dimeric form is 3.35 Å, and the opposing oxygen atoms are 2.39 Å apart. The cyclic 4-membered array is nearly planar with a Ti−O−Ti−O dihedral angle of 5.9°. Most importantly, the

https://doi.org/10.1021/acs.jpca.1c08447
J. Phys. Chem. A XXXX, XXX, XXX−XXX

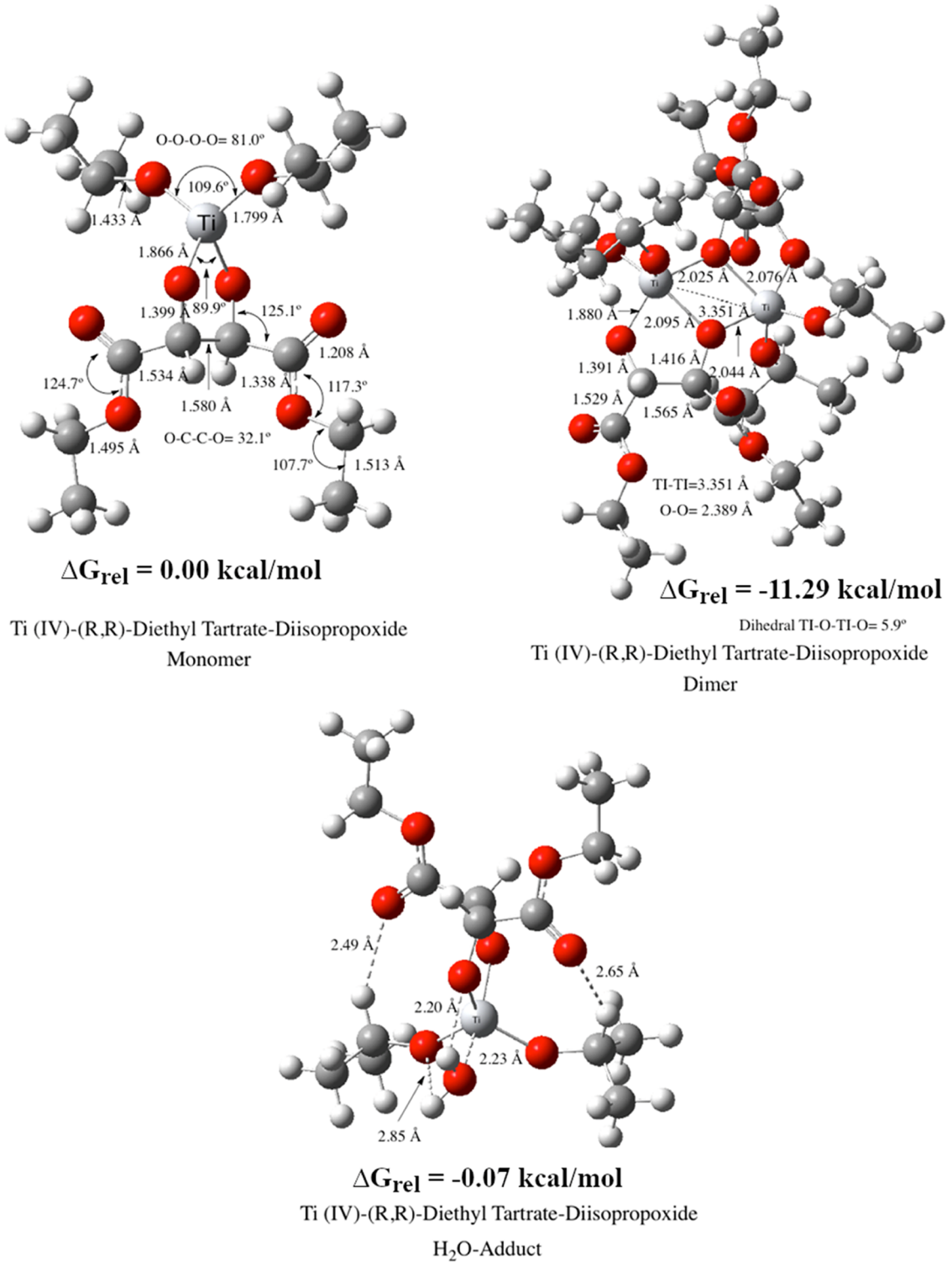

Figure 14. Dimerization of Ti(IV)-(R,R)-diethyl tartrate-diisopropoxide (B3LYP/6-311+G(d,p)) with dichloromethane solvent.

dimerization energy is $\Delta G = -11.28$ kcal/mol, providing a substantial impetus for dimerization. However, arriving at the global minimum for this dimer is problematic because the four ester functional groups can be arranged about the Ti−Ti bond with a number of different dihedral angles with respect to each other. In the dimer shown (Figure 14), the two C═O groups on each tartrate group are in a conformation with their O atoms opposed to each other. The bonding interactions of the C═O oxygen atom with the Ti centers are often represented with a dotted line (C═O···Ti), suggesting a favorable energy contribution to the overall energy. However, one Ti atom has a bonding distance for both carbonyl oxygens of 3.73 Å, while the other two O−Ti bonding distances to the other Ti atom are 5.49 and 5.97 Å. This does not support a strong bonding interaction between the two remaining C═O oxygen atoms and the Ti center. We have located several other closely related dimeric structures that are slightly higher in energy, largely due to minor changes in ester group nonbonding interactions.

https://doi.org/10.1021/acs.jpca.1c08447
J. Phys. Chem. A XXXX, XXX, XXX−XXX

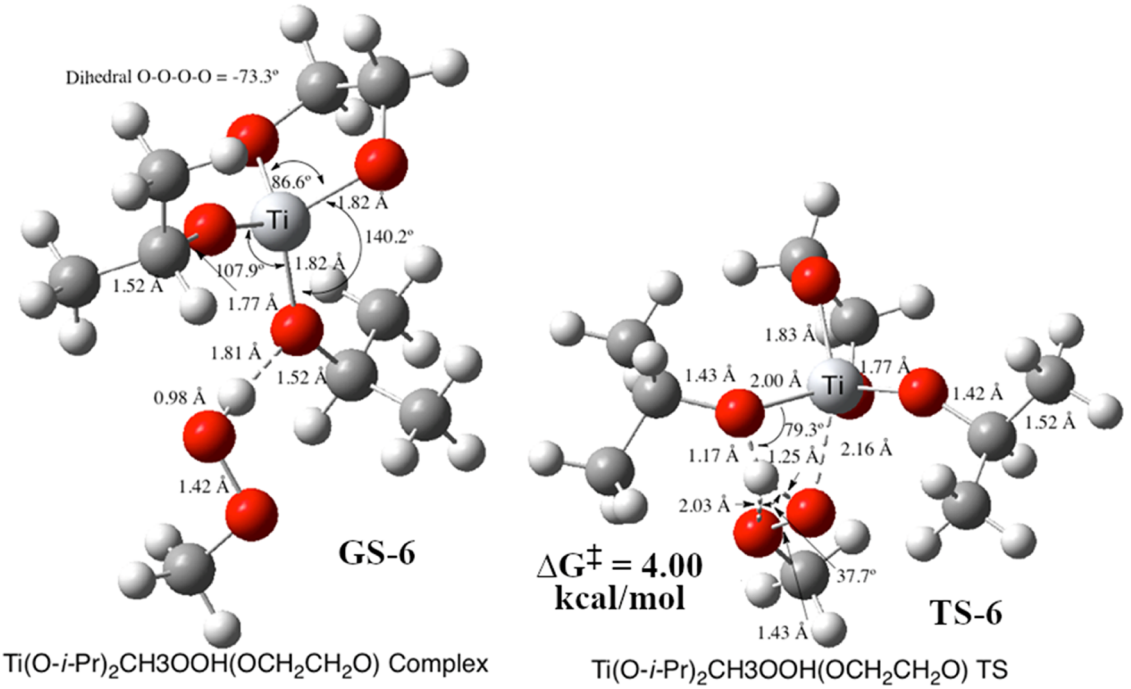

Figure 15. Ligand exchange methyl hydroperoxide for *i*-PrOH.

We also address the aforementioned effect that adventitious moisture present in the reaction mixture is the major source of poisoning of the Ti-tartrate catalytic moiety under reaction conditions in the Sharpless reaction. We therefore added a water molecule to the DET monomer (Figure 14) and find $\Delta H = -10.98$ kcal/mol for the binding of water to the Ti center. The Ti-OH_2 bond distance is 2.23 Å, and the H_2O hydrogens are hydrogen-bonded to the adjacent oxygens of the O-*i*-Pr ligand (2.85 Å) and the tartrate oxygen (2.20 Å). However, when we attempted to add a second H_2O to the Ti center, it failed to bind. The first H_2O remained firmly bound to the Ti center while the bonding distance of the second Ti-OH_2 was 3.5 Å and it was hydrogen-bonded to an adjacent carbonyl oxygen ($R_{C=O-Ti}$ = 1.9 Å). As noted above, spurious water has a marked effect upon the reactivity of H_2O_2-catalyzed epoxidation by bonding directly to the hydrophilic Ti(η^2-OOH) moiety.[14] In the present case, the H_2O bonds directly to the Ti center of the dimer effecting the dimerization equilibrium. The hydrolysis of the dimer with just two H_2O molecules is quite facile, $\Delta H = 4.46$ kcal/mol for the reaction: Dimer + $2H_2O \rightarrow 2(H_2O{-}Adduct)$ (Figure 14). Obviously, aqueous solvation of this monomeric form of the catalyst would have a deleterious effect upon its dimerization to produce the active precursor to the catalyst prior to ligand exchange. It is therefore conceivable that the presence of spurious water could also convert the dimer back to its monomeric stage resulting in the destruction of the effective dimeric epoxidation catalyst.

Ligand Exchange Reactions. It has been known for some time that Ti(O-*i*-Pr)$_4$ rapidly exchanges ligands, and this is a key feature that has rendered this asymmetric epoxidation reaction so successful. After the formation of the Ti-tartrate dimer, a statistical mixture of Ti species can arise from exchange of the isopropoxide ligands of the dimeric complex with *tert*-butyl hydroperoxide and the allyl alcohol substrates. This is a reversible reaction since both exchange reactions are fast when compared to that of the bidentate tartrate ligand. The explicit mechanistic steps in the ligand exchange process are not as well defined. However, DFT studies have shown the formation of titanium hydroperoxo intermediates involving hydroxyl ligand exchange with H_2O_2 to be quite involved.[12]

In Figure 15, we show the TS for our model reactant Ti(O-*i*-Pr)$_2$CH$_3$OOH(OCH$_2$CH$_2$O) exchanging its O-*i*-Pr alkoxide ligand with methyl hydroperoxide (CH_3O-OH). The pre-reaction complex for this exchange basically consists of CH_3O-OH hydrogen bonding to the oxygen atom of the incipient O-*i*-Pr leaving group with a relatively strong H bond (R_{OH} = 1.81 Å). The TS for this exchange is rather surprising because it consists almost entirely of the hydrogen from CH_3O-OH migrating to the Ti(O-*i*-Pr) oxygen. The migrating H atom in **TS-6** is approximately halfway between the two oxygens as evidenced by the very large imaginary frequency (ν_i = 1037*i*) attending light atom movement.[34] The peroxide OH bond has elongated to 1.25 Å, while the O−H bond to the O-*i*-Pr oxygen is comparable at 1.17 Å. In addition, the bonding of the migrating peroxide oxygen to the Ti atom is just starting to develop (R_{Ti-O} = 2.16 Å) as the isopropyl alkoxide ligand is starting to leave ($R_{Ti\text{-}O\text{-}i\text{-}Pr}$ = 2.00 Å). The activation barrier for this exchange reaction is relatively small consistent with a very rapid ligand exchange. The activation barrier is $\Delta G^{\ddagger}$ = 4.00 kcal/mol relative to the prereaction GS complex and $\Delta G^{\ddagger}$ = 6.73 kcal/mol when measured from isolated reactants. An IRC analysis clearly indicates the formation of the $CH_3O{-}O{-}Ti$ bond in the ligand exchange product. The equilibrium constants for the exchange of alkyl hydroperoxides for O-*i*-Pr ligands are sensitive to the steric environment of the titanium complex, especially in its dimeric form.

We also provide a transition state for ligand exchange involving *tert*-butyl hydroperoxide (Figure 16). Although initially we had anticipated a ligand exchange reaction involving an addition to the Ti center with displacement of the leaving O-*i*-Pr ligand, we again observe a TS that is largely involved with hydrogen transfer from the incoming hydroperoxide to the departing O-*i*-Pr alkoxide. The high imaginary

https://doi.org/10.1021/acs.jpca.1c08447
J. Phys. Chem. A XXXX, XXX, XXX−XXX

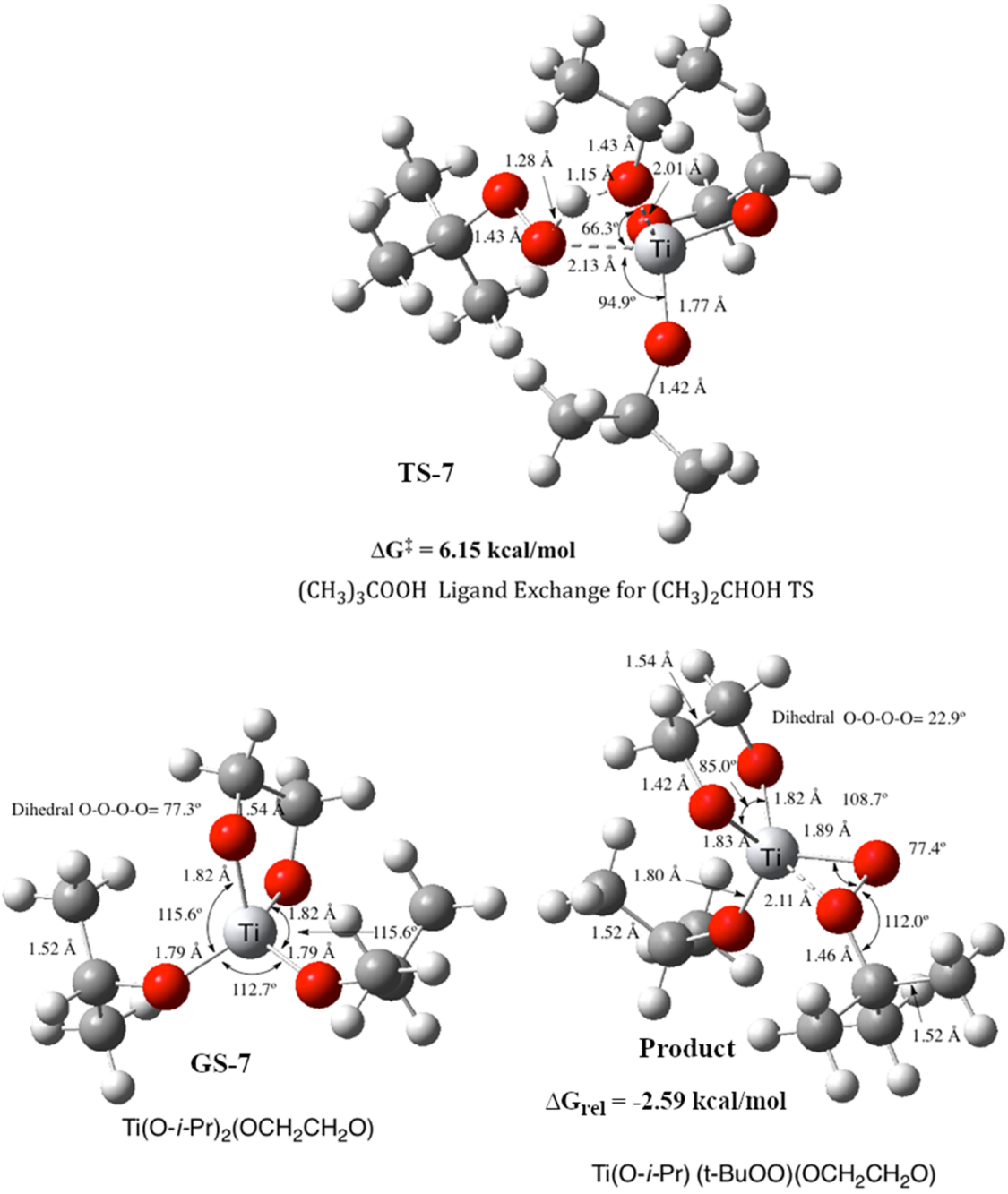

Figure 16. Ligand exchange *tert*-butyl hydroperoxide for *i*-PrOH.

frequency (ν_I = 991*i*) is again consistent with hydrogen migration. The transferring H atom is suspended between the two oxygens and has O−H bond distances of 1.28 and 1.15 Å. The departing O-*i*-Pr has a Ti−O bond distance of 2.01 Å relative to its typical GS bond distance of 1.77 Å. As anticipated, the O−O bond of the exchanging peroxide is quite typical at 1.43 Å. The Gibbs free energy of activation $\Delta G^{\ddagger}$ = 6.15 kcal/mol is still relatively low, and the overall Gibbs free energy of exchange is slightly negative (ΔG = −2.59 kcal/mol).

■ CONCLUSIONS

A model titanium(IV) hydroperoxo catalyst that employs *tert*-butyl hydroperoxide as the oxidant ($((CH_3O)_3TiO_p\text{-}O_dC\text{-}(CH_3)_3)$) can epoxidize E-2-butene with an activation barrier ($\Delta H^{\ddagger}$ = 15.40 kcal/mol) that is 7.20 kcal/mol lower than that observed with peroxyacetic acid. For peroxyacetic acid epoxidation, the O−O bond approaches the center of the carbon−carbon double bond in a linear fashion with a nearly spiro transition state. However, with Ti(IV)-catalyzed epoxidation of the allyl alcohol, the approach of the peroxide O−O bond deviates from linearity by about 15°. For epoxidation of E-2-butene, the Ti(IV) *tert*-butyl hydroperoxide catalyst is much more reactive than peroxyacetic acid ($\Delta\Delta H^{\ddagger}$ = 7.20 kcal/mol). When a water molecule is bound to the titanium atom in **GS-3** to achieve a hexacoordinate titanium peroxo environment, the barrier is decreased by 7.54 kcal/mol relative to a pentacoordinate Ti center. Rotation of the O−C−C═C dihedral angle to interconvert **GS-4a** and **GS-4b** has a very low barrier ($\Delta G^{\ddagger}$ = 4.11 kcal/mol). Curtain−Hammett considerations show that while the Gibbs free energy of

https://doi.org/10.1021/acs.jpca.1c08447
J. Phys. Chem. A XXXX, XXX, XXX−XXX

activation for epoxidation of these two ground states differs by only 0.24 kcal/mol, the Gibbs free energies of the transition states differ by 1.65 kcal/mol. When the (R,R)-(+)-diethyl tartrate chiral auxiliary is included in **GS-5a** and **GS-5b**, the barrier for the C−C bond rotation is $\Delta G^{\ddagger}$ = 3.67 kcal/mol and the Gibbs free energies of activation for epoxidation of allyl alcohol are 29.71 and 30.13 kcal/mol. The differences in these $\Delta\Delta G^{\ddagger}$ values for the two respective O−C−C═C dihedral angles are so small that one can largely exclude electronic factors in the oxygen atom transfer step as the source of the enantiomeric excess in the Sharpless epoxidation. Based on an energy difference of $\Delta\Delta G^{\ddagger}$ = 1.32 kcal/mol for the transition states, the product ratio should be about 97% for the desired enantiomer. Intramolecular oxygen atom transfer to a Ti-bound allylic alcohol involves transfer of the proximal oxygen to the C═C bond in a spiro orientation with a concomitant 1,3-migration of the *tert*-butoxide ligand to the Ti center in the TS. The ligand exchange of an *i*-PrOH group for *tert*-butyl hydroperoxide largely involves a hydrogen migration between two oxygen atoms of the interacting OH groups. The Gibbs free energy of activation for *tert*-butyl hydroperoxide displacement of the O-*i*-Pr alkoxide ($\Delta G^{\ddagger}$ = 6.15 kcal/mol) is relatively low, and the overall Gibbs free energy of exchange is slightly negative (ΔG = −2.59 kcal/mol). Evidence is provided to support the well-established concept that the Sharpless epoxidation involves the dimeric form of the catalyst based upon ΔG = −11.28 kcal/mol for the dimerization of Ti(IV)-(R,R)-diethyl tartrate-diisopropoxide. Since the $\Delta\Delta G^{\ddagger}$ for the typical Sharpless epoxidation is less than 2 kcal/mol, a detailed description of the atom motions required in the monomeric model will hopefully provide a better template for how this reaction transpires in the dimeric Sharpless catalyst.

■ ASSOCIATED CONTENT

Supporting Information

The Supporting Information is available free of charge at https://pubs.acs.org/doi/10.1021/acs.jpca.1c08447.

Total energies and Cartesian coordinates for all structures (PDF)

■ AUTHOR INFORMATION

Corresponding Author

Robert D. Bach − *Department of Chemistry and Biochemistry, University of Delaware, Newark, Delaware 19716, United States;* orcid.org/0000-0002-7331-5279; Email: rbach@udel.edu

Author

H. Bernhard Schlegel − *Department of Chemistry, Wayne State University, Detroit, Michigan 48202, United States;* orcid.org/0000-0001-7114-2821

Complete contact information is available at: https://pubs.acs.org/10.1021/acs.jpca.1c08447

Notes

The authors declare no competing financial interest.

■ ACKNOWLEDGMENTS

This work was supported, in part, by a grant from National Science Foundation (CHE1856437) to H.B.S. SEAGrid (http:www.seagrid.org) is acknowledged for computational resources and services for the selected results used in this publication. This work used the Extreme Science and Engineering Discovery Environment (XSEDE), which is supported by National Science Foundation (Grant Number OCI-1053575). The authors are particularly thankful to Dr. Sudhakar Pamidighantam for his assistance with the calculations carried out at SEAGRID.[35,36]

■ REFERENCES

(1) Joergensen, K. A. Transition-Metal-Catalyzed Epoxidation. *Chem. Rev.* **1989**, *89*, 431−457.

(2) Solé-Daura, A.; Zhang, T.; Fouilloux, H.; Robert, C.; Thomas, C. M.; Chamoreau, L.-M.; Carbo, J. J.; Proust, A.; Guillemot, G.; Poblet, J. M. Catalyst Design for Alkene Epoxidation by Molecular Analogues of Heterogeneous Titanium-Silicalite Catalysts. *ACS Catal.* **2020**, *10*, 4737−4750.

(3) Katsuki, T.; Sharpless, K. B. The First Practical Method for Asymmetric Epoxidation. *J. Am. Chem. Soc.* **1980**, *102*, 5974−5976.

(4) Finn, M. G.; Sharpless, K. B. Mechanism of Asymmetric Epoxidation. 2. Catalyst Structure. *J. Am. Chem. Soc.* **1991**, *113*, 113−126.

(5) Sharpless, K. B. Searching for New Reactivity (Nobel Lecture). *Angew. Chem., Int. Ed.* **2002**, *41*, 2024−2032.

(6) Bach, R. D. Structure and Mechanism for Alkane Oxidation and Alkene Epoxidation with Hydroperoxides, α-Hydroxy Peroxides and Peroxyacids. A Theoretical Study. *J. Phys. Chem. A* **2019**, *123*, 9520−9530.

(7) Bach, R. D. The Rate-Limiting Step in P450 Hydroxylation of Hydrocarbons. A Direct Comparison of the "Somersault" versus the "Consensus" Mechanism Involving Compound 1. *J. Phys. Chem. A* **2010**, *114*, 9319−9332.

(8) Bach, R. D.; Dmitrenko, O. Transient Inverted Metastable Iron Hydroperoxides in Fenton Chemistry. A Nonenzymatic Model for Cytochrome P450 Hydroxylation. *J. Org. Chem.* **2010**, *75*, 3705−3714.

(9) Özkılıç, Y.; Nurcan, T. S. Mechanism of Kynurenine 3-Monooxygenase-Catalyzed Hydroxylation Reaction: A Quantum Cluster Approach. *J. Phys. Chem. A* **2019**, *123*, 3149−3159.

(10) Wu, Y. D.; Lai, D. K. W. A Density Functional Study on the Stereocontrol of the Sharpless Epoxidation. *J. Am. Chem. Soc.* **1995**, *117*, 11327−11336.

(11) Wu, Y. D.; Lai, D. K. W. Transition Structure for the Epoxidation Mediated by Titanium(IV) Peroxide. A Density Functional Study. *J. Org. Chem.* **1995**, *60*, 673−680.

(12) Sever, R. R.; Root, T. W. DFT Study of Solvent Coordination Effects on Titanium-Based Epoxidation Catalysts. Part Two: Reactivity of Titanium Hydroperoxo Complexes in Ethylene Epoxidation. *J. Phys. Chem. B* **2003**, *107*, 4090−4099.

(13) Antonova, N. S.; Carbo, J. J.; Kortz, U.; Kholdeeva, O. A.; Poblet, J. M. Mechanistic Insights into Alkene Epoxidation with H_2O_2 by Ti- and other TM-Containing Polyoxometalates: Role of the Metal Nature and Coordination Environment. *J. Am. Chem. Soc.* **2010**, *132*, 7488−7497.

(14) Jiménez-Lozano, P.; Ivanchikova, I. D.; Kholdeeva, O. A.; Poblet, J. M.; et al. Alkene Epoxidation by Ti-Containing Polyoxometalates. Unambiguous Characterization of the Role of the Protonation State. *Chem. Commun.* **2012**, *48*, 9266−9268.

(15) Jiménez-Lozano, P.; Skobelev, I. Y.; Kholdeeva, O. A.; Poblet, J. M.; Carbo, J. J. Epoxidation Catalyzed by Ti-Containing Polyoxometalates: Unprecedented β-Oxygen Transfer Mechanism. *Inorg. Chem.* **2016**, *55*, 6080−6084.

(16) Cui, M.; Adam, W.; Shen, J. H.; Luo, X. M.; Tan, X. J.; Chen, K. X.; Ji, R. Y.; Jiang, H. J. A Density-Functional Study of the Mechanism for the Diastereoselective Epoxidation of Chiral Allylic Alcohols by the Titanium Peroxy Complexes. *J. Org. Chem.* **2002**, *67*, 1427−1435.

(17) Frisch, M. J.; Trucks, G. W.; Schlegel, H. B.; Scuseria, G. E.; Robb, M. A.; Cheeseman, J. R.; Scalmani, G.; Barone, V.; Mennucci,

B.; Petersson, G. et al. *Gaussian 16*, revision B.01; Gaussian Inc.: Wallingford, CT, 2019.
(18) Schlegel, H. B. Geometry Optimization. *WIREs Comput. Mol. Sci.* **2011**, *1*, 790−809.
(19) Zhao, Y.; Truhlar, D. G. The M06 suite of density functionals for main group thermochemistry, thermochemical kinetics, noncovalent interactions, excited states, and transition elements: two new functionals and systematic testing of four M06-class functionals and 12 other functionals. *Theor. Chem. Acc.* **2008**, *120*, 215−241.
(20) Becke, A. D. Density-Functional Exchange-Energy Approximation with Correct Asymptotic Behavior. *Phys. Rev. A* **1988**, *38*, 3098−3100.
(21) Becke, A. D. Density - Functional Thermochemistry. III. The Role of Exact Exchange. *J. Chem. Phys.* **1993**, *98*, 5648−5652.
(22) Bach, R. D.; Ayala, P. Y.; Schlegel, H. B. A Reassessment of the Bond Dissociation Energies of Peroxides. *J. Am. Chem. Soc.* **1996**, *118*, 12758−12765.
(23) Bach, R. D.; Schlegel, H. B. Bond Dissociation Energy of Peroxides Revisited. *J. Phys. Chem. A* **2020**, *124*, 4742−4751.
(24) Bach, R. D.; Schlegel, H. B. The Bond Dissociation Energy of the N-O Bond. *J. Phys. Chem. A* **2021**, *125*, 5014−5021.
(25) Bach, R. D.; Wolber, J. G.; Coddens, B. A. On the Mechanism of Metal-Catalyzed Epoxidation. A Model for the Bonding in Peroxo-Metal Complexes. *J. Am. Chem. Soc.* **1984**, *106*, 6098−6099.
(26) Bach, R. D.; Dmitrenko, O. Spiro versus Planar Structures in the Epoxidation of Simple Alkenes. A Reassessment of the Level of Theory Required. *J. Phys. Chem. A* **2003**, *107*, 4300−4306.
(27) Chong, A. O.; Sharpless, K. B. On the Mechanism of the Molybdenum and Vanadium Catalyzed Epoxidation of Olefins by Alkyl Hydroperoxides. *J. Org. Chem.* **1977**, *42*, 1587−1590.
(28) Schneebeli, S. T.; Hall, M. L.; Breslow, R.; Friesner, R. J. Quantitative DFT Modeling of the Enantiomeric Excess for Dioxirane-Catalyzed Epoxidations. *J. Am. Chem. Soc.* **2009**, *131*, 3965−3973.
(29) Sever, R. R.; Root, T. W. DFT Study of Solvent Coordination Effects on Titanium-Based Epoxidation Catalysts. Part One: Formation of the Titanium Hydroperoxo Intermediate. *J. Phys. Chem. B* **2003**, *107*, 4080−4089.
(30) Seeman, J. I. The Curtin-Hammett Principle and the Winstein-Holness Kinetics. *J. Chem. Educ.* **1986**, *63*, 42−48.
(31) Morgans, D. J., Jr.; Sharpless, K. B.; et al. Epoxy Alcohol Rearrangements: Hydroxyl-mediated Delivery of Lewis Acid Promoters. *J. Am. Chem. Soc.* **1981**, *103*, 462−464.
(32) Williams, I. D.; Pedersen, S. F.; Sharpless, K. B.; Lippard, S. J. Crystal-Structures of 2 Titanium Tartrate Asymmetric Epoxidation Catalysts. *J. Am. Chem. Soc.* **1984**, *106*, 6430−6431.
(33) (a) Hanson, R. M.; Sharpless, K. B. Procedure for the Catalytic Asymmetric Epoxidation of Allylic Alcohols in the presence of Molecular Sieves. *J. Org. Chem.* **1986**, *51*, 1922−1925. (b) Fernandes, A. S.; Maitre, P.; Correra, T. C. Evaluation of the Katsuki-Sharpless Epoxidation Precatalysts by ESI-FTMS, CID, and IRMPD Spectroscopy. *J. Phys. Chem. A* **2019**, *123*, 1022−1029.
(34) Contrariwise, when the reaction vector consists mainly of heavy-atom OH motion as in peracid alkene epoxidation, the single negative imaginary frequency of the first-order saddle point is only about 300*i* to 600*i* cm^{-1}; when the reaction vector is composed mostly of light-atom hydrogen motion, the imaginary frequency is typically as high as 1200*i* cm^{-1}. Bach, R. D.; Dmitrenko, O. Electronic Requirements for Oxygen Atom Transfer from Alkyl Hydroperoxides. Model Studies on Multisubstrate Flavin-Containing Monooxygenases. *J. Phys. Chem. B* **2003**, *107*, 12851−12861.
(35) Pamidighantam, S.; Nakandala, S.; Abeysinghe, E.; Wimalasena, C.; Yodage, S. R.; Marru, S.; Pierce, M. Community Science Exemplars in SEAGrid Science Gateway: Apache Airavata Based Implementation of Advanced Infrastructure. *Procedia Comput. Sci.* **2016**, *80*, 1927−1939.
(36) Shen, N.; Fan, Y.; Pamidighantam, S. E-Science Infrastructures for Molecular Modeling and Parametrization. *J. Comput. Sci.* **2014**, *5*, 576−589.

https://doi.org/10.1021/acs.jpca.1c08447
J. Phys. Chem. A XXXX, XXX, XXX−XXX